

This Prospectus for a Dissertation
entitled
PLASMA FLOW CONTROL
FOR NOISE REDUCTION
ON A G550 NOSE LANDING GEAR

typeset with $\text{NDDiss2}_{\mathcal{E}}$ v3.2013 (2013/04/16) on December 8, 2015 for

Michael C. Wicks

This $\text{\LaTeX} 2_{\mathcal{E}}$ classfile conforms to the University of Notre Dame style guidelines as of Fall 2012. However it is still possible to generate a non-conformant document if the instructions in the class file documentation are not followed!

Be sure to refer to the published Graduate School guidelines at <http://graduateschool.nd.edu> as well. Those guidelines override everything mentioned about formatting in the documentation for this $\text{NDDiss2}_{\mathcal{E}}$ class file.

It is YOUR responsibility to ensure that the Chapter titles and Table caption titles are put in CAPS LETTERS. This classfile does *NOT* do that!

*This page can be disabled by specifying the “noinfo” option to the class invocation.
(i.e., \documentclass[. . . , noinfo] {nddiss2e})*

This page is *NOT* part of the dissertation/thesis. It should be disabled before making final, formal submission, but should be included in the version submitted for format check.

$\text{NDDiss2}_{\mathcal{E}}$ documentation can be found at these locations:

<http://www.gsu.nd.edu>
<http://graduateschool.nd.edu>

PLASMA FLOW CONTROL
FOR NOISE REDUCTION
ON A G550 NOSE LANDING GEAR

A Prospectus for a Dissertation

Submitted to the Graduate School
of the University of Notre Dame
in Partial Fulfillment of the Requirements
for the Degree of

Doctor of Philosophy

by
Michael C. Wicks

Flint O. Thomas, Director

Graduate Program in Aerospace and Mechanical Engineering

Notre Dame, Indiana

December 2015

© Copyright by
Michael C. Wicks
2015
All Rights Reserved

PLASMA FLOW CONTROL
FOR NOISE REDUCTION
ON A G550 NOSE LANDING GEAR

Abstract

by

Michael C. Wicks

Please note that the full \LaTeX source code (and an associated `Makefile`) is available from the University of Notre Dame Graduate Student Union web site. The Information Technology Committee page¹ has all the necessary files in download-able form. This particular dissertation was developed under Unix, but is also be usable under Windows with the appropriate \LaTeX setup and was modified on a Windows system in 2012-2013. It should also work with on Mac.

While the source code for this document provides an excellent example for how to use the `NDdiss2 ε` \LaTeX class to write a Notre Dame thesis, it is *not* a substitution for the documentation of the `NDdiss2 ε` \LaTeX class (also available on the ND GSU web site).

In this thesis, I will tell all that I know about Gnus. Gnus are wonderful little creatures that inhabit the center of the earth and give us wonderful and plentiful trees, dirt, and other earthly-things.

In short, we should love and cherish the Gnus. They can be very friendly, and are often mistaken for squirrels on the University of Notre Dame campus. Feed them

¹<http://www.gsu.nd.edu/>

whenever possible. If they get caught in trash cans, tip them over so that they can get out.

This abstract is going to continue on, including a few formulas, just for the sake of spilling over on to two pages so that we can see the author's name in the top right corner:

$$a^2 + b^2 = c^2$$

$$E = mc^2$$

$$\frac{e}{m} = c^2$$
$$a^2 + b^2 = \frac{e}{m}$$

These equations, by themselves mean nothing. But to the common Gnu, they define a whole way of living. While intricate mathematical implications certainly do not infiltrate the majority of humans' lives, every Gnu, from birth, is imbued with a sense of mathematical certainty and guidance. All Gnus, great and small, feel at one with mathematics. The cute furry bit is just a scam for their calculating minds.

To Laurimar

CONTENTS

FIGURES	iv
TABLES	v
CHAPTER 1: INTRODUCTION	1
1.1 Motivation	1
1.2 Theory of Aeroacoustics	1
1.3 Landing Gear	6
1.3.1 Geometry	6
1.3.2 Noise Sources	6
1.4 Literature Review	6
1.4.1 Single Cylinder Plasma Flow Control	6
1.4.2 Tandem Cylinders Plasma Flow Control	6
1.4.3 Shock Strut-Torque Arm Assembly Plasma Flow Control	6
CHAPTER 2: EXPERIMENTAL APPROACH	9
2.1 Experimental Objective	9
2.2 Experimental Facility	9
2.3 Notre Dame G550 Nose Landing Gear Model	9
2.4 Flow Visualization	11
2.5 Pressure Measurements	11
2.6 Microphone Measurements	11
2.7 Data Acquisition	11
2.8 Current Results	13
CHAPTER 3: OBJECTIVES AND FUTURE WORK	14
3.1 Research Objectives	14
3.2 Proposed Future Work	14
3.3 Conclusion	14

FIGURES

1.1	Photograph of Gulfstream 550 Nose Landing Gear	4
1.2	Schematic view of Gulfstream 550 Nose Landing Gear components . .	5
1.3	Flow Visualization of single cylinder in cross-flow with Spanwise and PSVG plasma actuators.	6
1.4	Flow Visualization of tandem cylinders in cross-flow with Spanwise and PSVG plasma actuators.	7
1.5	Flow Visualization of torque-arm assembly in cross-flow with Spanwise plasma actuators.	8
2.1	ND G550 model with and without plasma fairing installed.	10
2.2	Schematic of the polar array.	12
2.3	Photograph of the polar array installed in the ND AWT.	12

TABLES

2.1 Data acquisition parameters. 13

CHAPTER 1

INTRODUCTION

Airframe noise is significant

Landing gear is primary source of airframe noise

Health risks

1.1 Motivation

The present work is motivated to reduce noise by flow control via application of DBD plasma actuator technology.

In this chapter, the physics of airframe noise production is discussed. The structure of Aircraft landing gear is presented. This geometry is grouped into two main sub-systems which can be considered for flow-control separately. Areas of noise contribution are considered and the underlying physical mechanisms are discussed. Finally, the literature is reviewed with respect to the application of Plasma Flow Control to increasingly complex geometries.

1.2 Theory of Aeroacoustics

The modern theory of aeroacoustics, that is sound generated by aerodynamic means, is based on James Lighthill's so-called acoustic analogy. He states that sound generated in a fluid flow is only important in regions of turbulent fluctuations [?]. Based on this assumption, the Navier-Stokes Equation and isentropic equation of state are

$$\frac{\partial \rho}{\partial t} + \frac{\partial(\rho u_i)}{\partial x_i} = 0 \quad (1.1)$$

$$\frac{\partial(\rho u_i)}{\partial t} + \frac{\partial(\rho u_i u_j + P_{ij})}{\partial x_j} = 0 \quad (1.2)$$

$$c_o^2 = \frac{\partial p}{\partial \rho}|_{s=const.} = \frac{p'}{\rho'}. \quad (1.3)$$

$$\frac{\partial^2 \rho}{\partial t^2} - c_o^2 \nabla^2 \rho = \frac{\partial^2 T_{ij}}{\partial x_i \partial x_j}. \quad (1.4)$$

$$T_{ij} = \rho u_i u_j + P_{ij} - c_o^2 (\rho - \rho_0) \delta_{ij}, \quad (1.5)$$

where

$$\delta_{ij} = \begin{cases} 1 & \text{if } i = j \\ 0 & \text{if } i \neq j \end{cases} \quad (1.6)$$

$$T_{ij} \approx \rho_0 u_i u_j. \quad (1.7)$$

$$p' = c_o^2 \rho' = \frac{1}{4\pi} \frac{\partial^2}{\partial x_i \partial x_j} \int_V \frac{T_{ij}}{r} dV, \quad (1.8)$$

$$\int_V dV \propto D^3 \quad (1.9)$$

$$T_{ij} \propto \rho_o U_o^2 \quad (1.10)$$

$$\frac{\partial}{\partial x_i} = \frac{\partial}{c_o \partial t} \propto \frac{f}{c_o} \propto \frac{U_o}{c_o D} \quad (1.11)$$

$$p' \propto \left(\frac{U_o}{c_o D} \right)^2 (D^3) \left(\frac{\rho_o U_o^2}{r} \right) \propto \frac{U_o^4}{r} \quad (1.12)$$

$$W \propto p'^2 \propto \frac{U_o^8}{r^2} \quad (1.13)$$

$$\begin{aligned} p' &= \underbrace{\frac{1}{4\pi} \frac{\partial^2}{\partial x_i \partial x_j} \int_V \left[\frac{T_{ij}}{r} \right] dV}_I - \underbrace{\frac{1}{4\pi} \frac{\partial}{\partial x_j} \int_S \left[\frac{P_{ij} + \rho v_i v_j}{r} \right] n_i dS}_{II} \\ &\quad + \underbrace{\frac{1}{4\pi} \frac{\partial}{\partial t} \int_S \left[\frac{\rho v_i}{r} \right] n_i dS}_{III}, \end{aligned} \quad (1.14)$$

$$II : \frac{1}{4\pi} \frac{\partial}{\partial x_j} \int_S \left[\frac{P_{ij} + \rho v_i v_j}{r} \right] n_i dS \propto \left(\frac{U_o}{c_o D} \right) \left(\frac{\rho_o U_o^2}{r} \right) (D^2) \propto \frac{U_o^3}{r} \quad (1.15)$$

$$III : \frac{1}{4\pi} \frac{\partial}{\partial t} \int_S \left[\frac{\rho v_i}{r} \right] n_i dS \propto \left(\frac{U_o}{D} \right) \left(\frac{\rho_o U_o}{r} \right) (D^2) \propto \frac{U_o^2}{r}. \quad (1.16)$$

$$II : W \propto p'^2 \propto \frac{U_o^6}{r^2}, \quad (1.17)$$

$$III : W \propto p'^2 \propto \frac{U_o^4}{r^2}. \quad (1.18)$$



Figure 1.1. Photograph of Gulfstream 550 Nose Landing Gear

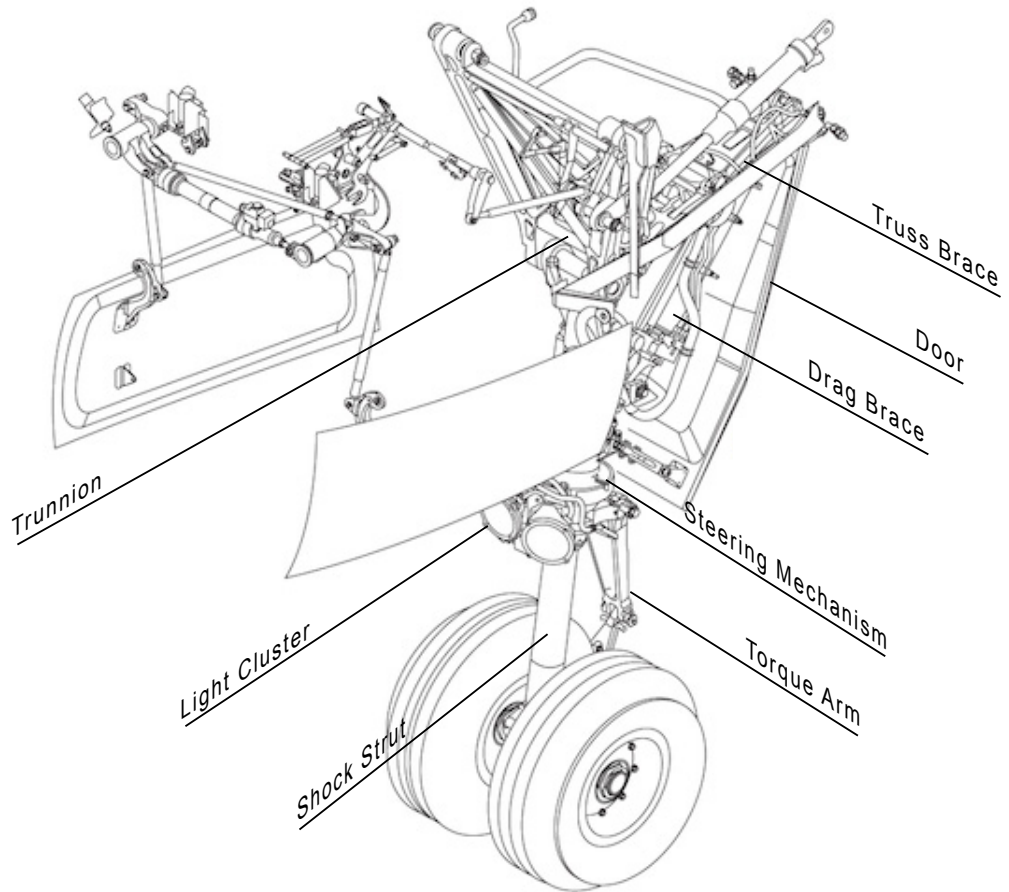


Figure 1.2. Schematic view of Gulfstream 550 Nose Landing Gear components

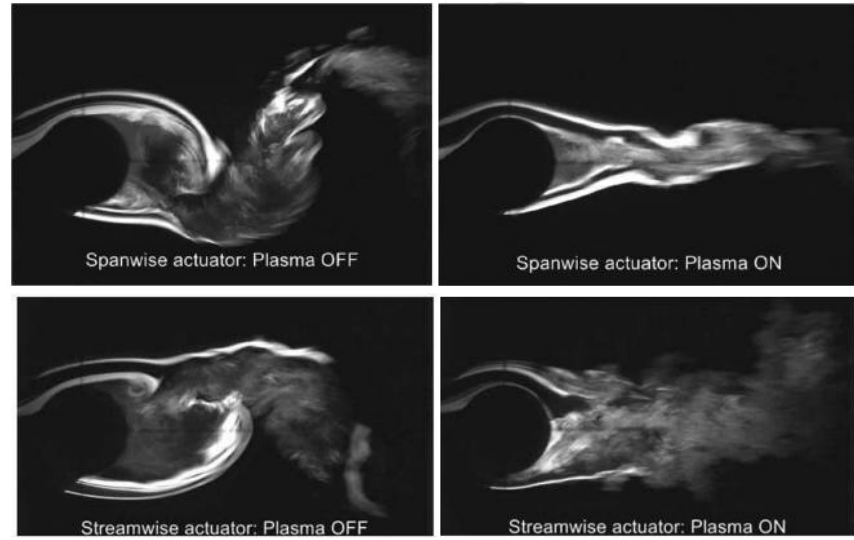


Figure 1.3. Flow Visualization of single cylinder in cross-flow with Spanwise and PSVG plasma actuators.

1.3 Landing Gear

1.3.1 Geometry

1.3.2 Noise Sources

1.4 Literature Review

1.4.1 Single Cylinder Plasma Flow Control

1.4.2 Tandem Cylinders Plasma Flow Control

1.4.3 Shock Strut-Torque Arm Assembly Plasma Flow Control

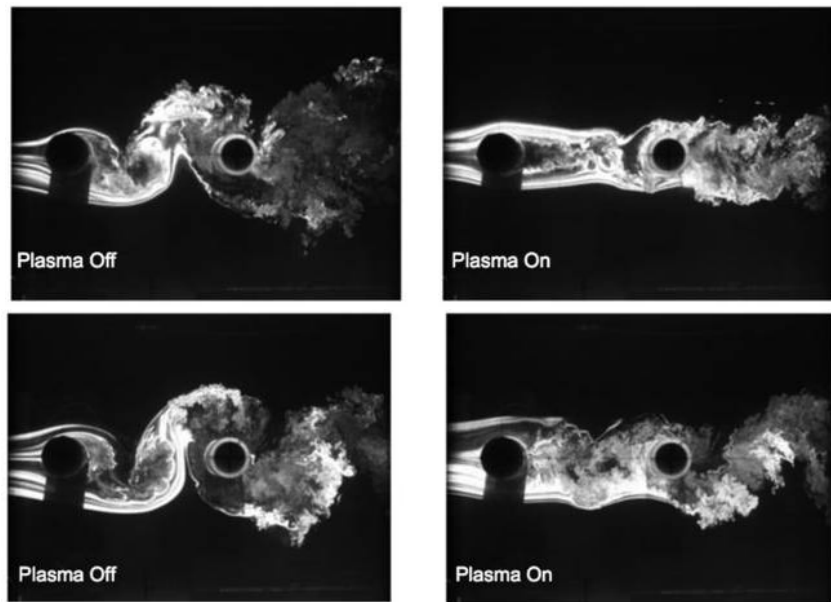


Figure 1.4. Flow Visualization of tandem cylinders in cross-flow with Spanwise and PSVG plasma actuators.

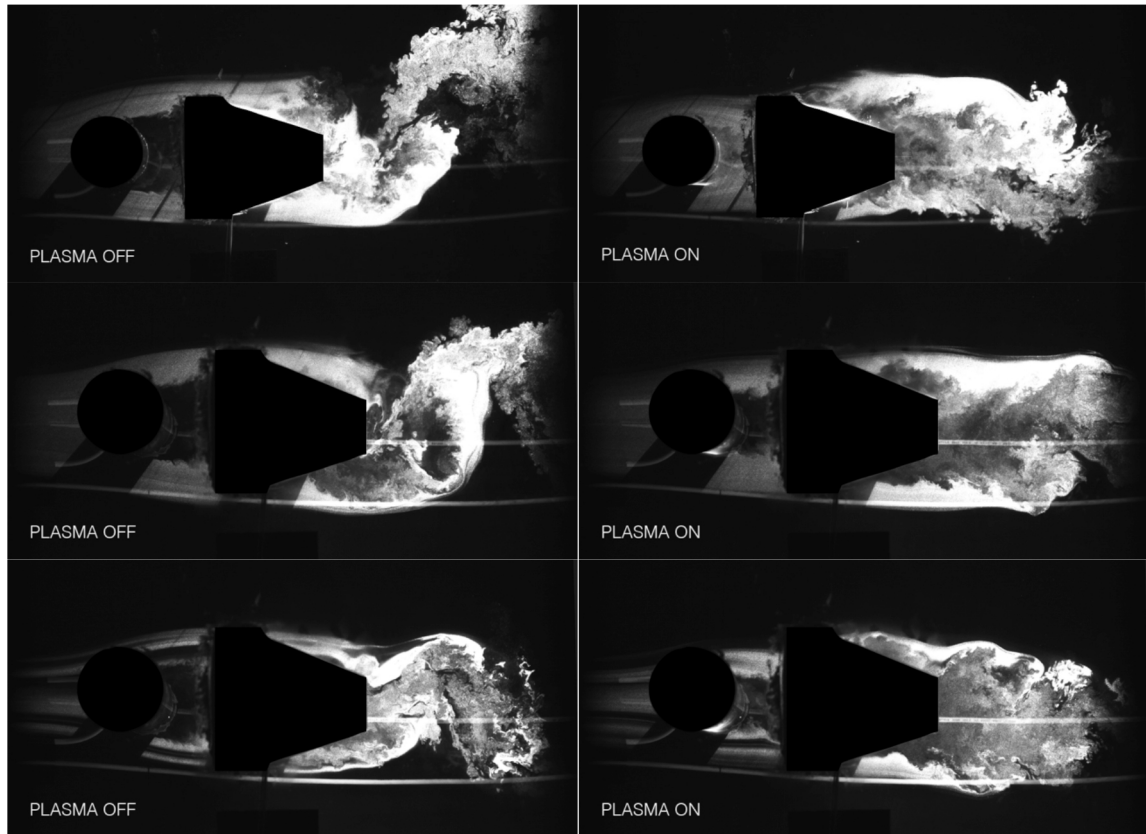


Figure 1.5. Flow Visualization of torque-arm assembly in cross-flow with Spanwise plasma actuators.

CHAPTER 2

EXPERIMENTAL APPROACH

2.1 Experimental Objective

2.2 Experimental Facility

Baseline acoustic measurements without plasma flow control were obtained in the Notre Dame Anechoic Wind Tunnel Facility (ND AWT). The ND AWT is a low-noise, open-jet acoustic wind tunnel with a free jet test section measuring 24-in-(0.610 m)-high by 24-in-(0.610 m)-wide installed in a large anechoic chamber suitable for frequencies above 100 Hz. The maximum empty test section velocity is approximately $U_\infty = 35$ m/s. The maximum safe tunnel velocity with the Notre Dame G550 Nose Landing Gear 30%-scale model (ND G550) installed is 30 m/s corresponding to a Mach number of $M_\infty = 0.1$.

Atmospheric properties such as ambient temperature and pressure were acquired using a digital thermometer and barometer. The tunnel speed is measured using a pitot-static probe installed approximately 6 in (0.154 m) from the free jet inlet centerline. From these data local sonic speed and the flow Mach number is computed.

2.3 Notre Dame G550 Nose Landing Gear Model

Acoustic measurement for two baseline landing gear model configurations were performed. The first, designated Baseline 1, consisted of the ND G550 model without the plasma fairing installed, which is shown in the photograph of Figure 2.1a. The second, designated Baseline 2, involved the ND G550 model retrofitted with a plasma



(a) Baseline 1



(b) Baseline 2

Figure 2.1. ND G550 model with and without plasma fairing installed.

fairing assembly in order to facilitate installation of dielectric barrier discharge (DBD) plasma actuators for flow control. This configuration is shown in the photograph of Figure 2.1b. None of the acoustic measurements presented in this report for both configurations involved the use of plasma flow control. Rather, the focus was on the characterization of baseline acoustics for both configurations.

2.4 Flow Visualization

2.5 Pressure Measurements

2.6 Microphone Measurements

A polar array of omnidirectional microphones was used to acquire far field noise level spectra along the length of the AWT test section. It consists of a 1/2-in ACO Model 7046 electret microphone with companion 4012 preamplifier and PS9200 power supply. A schematic illustrating the array is shown in Figure 2.2. Additionally, the array configuration relative to the G550 model is shown in the photograph of Figure 2.3. The microphone is mounted using a microphone stand so as to protrude from an acoustically treated rail by approximately 13 in (0.330 m). The total range of acoustic source-to-microphone angle spanned by the polar array is approximately $30^\circ \leq \theta \leq 150^\circ$ as referenced from the upper torque arm of the model in the downstream flow direction. As shown in Figure 2.3, the polar array is situated along the length of the free jet test section and positioned at the same height as the upper torque arm of the model, with the plane of the microphone located approximately 59 in (1.50 m) from the test section centerline.

2.7 Data Acquisition

For microphone data acquisition, a National Instruments USB-6343 DAQ was used, yielding a total of 45 available channels with 48-bit ADC. The sampling pa-

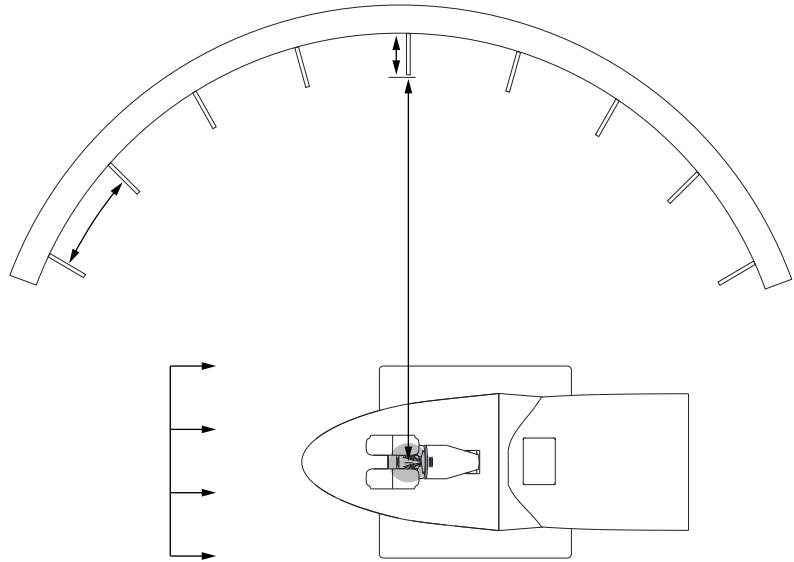


Figure 2.2. Schematic of the polar array.

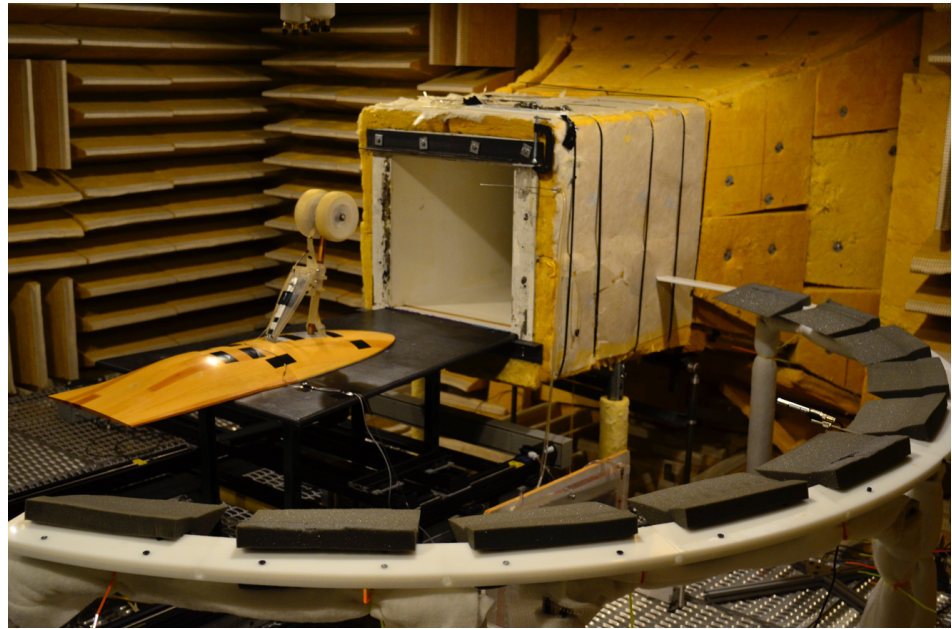


Figure 2.3. Photograph of the polar array installed in the ND AWT.

TABLE 2.1

Data acquisition parameters.

Sensors	Sampling Rate (Hz)	$\frac{Samples}{block}$	Window Function	Overlap (%)	N_{blocks}	$N_{averages}$	Acquisition Time (s)
ACO	65,536	2048	Hanning	0	960	960	30

rameters for the microphone data acquisition are listed in Table 2.1.

2.8 Current Results

CHAPTER 3

OBJECTIVES AND FUTURE WORK

3.1 Research Objectives

3.2 Proposed Future Work

3.3 Conclusion

*This document was prepared & typeset with pdfL^AT_EX, and formatted with
NDdiss2_ε classfile (v3.2013[2013/04/16]) provided by Sameer Vijay and updated
by Megan Patnott.*